inorganics

MDPI

Article

Characterization of Boron-Modified Activated Carbons

Ayhan Orhan [1], Nurettin Çek [2,3,*], Selman Sezer [4] and Ismail Demir [5]

[1] Department of Metallurgical and Materials Engineering, Faculty of Technology, Firat University, 23119 Elazig, Turkey; ayorhan@firat.edu.tr
[2] Department of Metallurgical and Materials Engineering Technology, Graduate School of Natural and Applied Sciences, Firat University, 23119 Elazig, Turkey
[3] Department of Machinery and Metal Technologies, Vocational School, Ostim Technical University, 06374 Ankara, Turkey
[4] Department of Mechatronics Engineering, Graduate School of Natural and Applied Sciences, Firat University, 23119 Elazig, Turkey; sesezer07@gmail.com
[5] Karabuk Iron and Steel Factories (KARDEMİR) Inc., 78170 Karabuk, Turkey
* Correspondence: nurettincek001@gmail.com or nurettin.cek@ostimteknik.edu.tr

Abstract: Although there are various boron production methods for modified activated carbons used in sulfur removal, catalyst synthesis, and hydrogen capture/storage processes, the modification of activated carbon with borax solutions has attracted attention as the easiest synthesis method. However, structural characterization analyses in previous studies contradict each other and, therefore, more detailed characterization is needed. In this study, 0.25 M and 0.5 M borax solutions are prepared in distilled water; then, 2 g of commercial activated carbon is added to each one, mixed at 60 °C, filtered, and dried. Thus, two different boron-modified activated carbon materials are obtained. Structural characterization tests of these materials are performed and analyzed by comparing with the literature. As a result, two different boron-modified activated carbon structural analyzes are compared and it is confirmed that commercially activated carbon material induced phase composition and chemical bond modification as a result of modification with borax. It is revealed that the induction of phase composition and chemical bond modification is more dominant with increasing borax concentration. The produced boron-modified activated carbon materials have great promise for the development of new technologies in the fields of the environment, energy, lightweight compressible materials, thermal insulation, and composite materials.

Keywords: carbon materials; commercial activated carbon; borax; boron; modification

check for updates

Academic Editors: Michael A. Beckett and Pingwu Du

Received: 19 January 2025
Revised: 10 February 2025
Accepted: 11 February 2025
Published: 13 February 2025

Citation: Orhan, A.; Çek, N.; Sezer, S.; Demir, I. Characterization of Boron-Modified Activated Carbons. *Inorganics* **2025**, *13*, 54. https://doi.org/10.3390/inorganics13020054

Copyright: © 2025 by the authors. Licensee MDPI, Basel, Switzerland. This article is an open access article distributed under the terms and conditions of the Creative Commons Attribution (CC BY) license (https://creativecommons.org/licenses/by/4.0/).

1. Introduction

Carbon-based materials are constantly finding new applications in scientific and industrial processes. As an example, the boron doping of carbon materials was investigated in 2013 to obtain a high hydrogen storage capacity and reduce the limitation of the physical adsorption of hydrogen. In the study, boron-doped activated carbon was obtained by two different methods. In the first one, boron-doped activated carbon was synthesized by mixing activated carbon obtained from corn cob biomass with decaborane ($B_{10}H14$) material and degassing it in a reaction cell at −30 °C in a vacuum for 1 h and then keeping the mixture in vacuum. In the second one, boron-doped activated carbon was synthesized by mixing commercial boron carbide material with potassium hydroxide and subjecting it to heat treatment [1]. In another study, boron-doped activated carbon was prepared by heating, mixing and drying commercial activated carbon in boric acid solution to

remove sulfur from 4,6-dimethyldibenzothiophene (4,6-DMDBT) material. The results of the study revealed that the boron-doped activated carbon showed selectivity towards the complex refractory organosulfur compound (4,6-DMDBT) and was effective in significantly removing sulfur from the model fuel [2]. In another study, after various treatments of boric acid and activated carbon materials, the sample was dried and calcined under nitrogen at 500 °C for 5 h to obtain boron-doped activated carbon. Then, using the wet impregnation technique, chloroauric acid solution ($HAuCl_4 \cdot H_2O$) dissolved in ethanol was impregnated onto the boron-doped activated carbon and dried. Thus, boron-modified activated carbon supporting gold-based catalysts was synthesized. In the same study, it was observed that the obtained catalyst material increased acetylene conversion and vinyl chloride selectivity. In addition, it was observed that boron addition increased the adsorption of hydrochloric acid (HCl) reactant and the number of active species in acetylene hydrochlorination, and as a result, it was understood that catalyst stability was improved [3].

The boron-modified (doped) activated carbon material, which was investigated for use in hydrogen adsorption applications, was obtained by treating bituminous coal with potassium hydroxide then adding borax decahydrate material and following a chemical activation process. The results of the study show that boron-modified activated carbons were successfully prepared from coal samples using a mixed combination of potassium hydroxide (KOH) and borax decahydrate and subjected to a chemical activation process [4].

In order to perform hydrogen adsorption more effectively, the activated carbons obtained after treating the coal with KOH activation were further modified with ammonia and, finally, the samples were further modified with borax decahydrate and ammonia–boron-modified activated carbon material was obtained. Here, the irregularity of the forms of the produced samples revealed the need for a more detailed characterization of boron-modified activated carbons [5]. In the study conducted to discover an effective electrocatalyst in the electrochemical advanced oxidation process, which is a method applied to enhance the degradation of persistent organic pollutants, the boron-doped activated carbon obtained using commercial activated carbon and boron compounds (boric acid, etc.) was called boride-activated carbon. The results of the study showed that low-cost, effective catalysts were revealed, providing a theoretical basis for the further application of the boron catalyst [6]. In a recent study investigating hydrogen storage, boron-modified activated carbon was obtained using commercial activated carbon and borax decahydrate using the wet impregnation technique in demineralized water [7]. The results obtained from the study contradict the results obtained from boron-modified activated carbon material reported in previous studies [5]. Moreover, although X-ray diffraction analysis (XRD), which provides information about the structure of the materials, showed the structure of sodium boron hydroxide hydrate, the findings could not be associated with the textural properties [7]. Therefore, the findings obtained are scientifically insufficient and need further comparison and research. Table 1 provides a summary of the production methods of boron-modified activated carbon materials.

Since different processes and additives are used in the preparation process of boron-modified activated carbons, the differences in structural characterization tests are remarkable. In addition, the absence of more than one test parameter in the characterization tests of purple-modified activated carbons and the inability to establish their relationships with each other continue to be important deficiencies. In order to eliminate these deficiencies, boron-modified activated carbon was synthesized in aqueous solution using commercial activated carbon material and borax decahydrate in this study. The obtained material was characterized by XRD, Fourier Transform Infrared Spectroscopy (FTIR), Raman and Field Emission Scanning Electron Microscopy (FESEM)–Energy Dispersive Spectrometry (EDS) tests and its structural characterization was carried out. Thus, the detailed information

and properties of borax-modified activated carbons were better known with structural characterization tests. In this way, this study will be a better source of ideas for future scientific or industrial-scale studies.

Table 1. Production methods of boron-modified activated carbons.

Reaction Materials	Reaction Medium	Reference
Activated carbon from corn cob + decaborane	In vacuum at −30 °C	[1]
Boron carbide + potassium hydroxide	Heat treatment at 790 °C for 1 h	[1]
4,6-dimetildibenzotiofen + boric acid	Calcination at 600 °C in N_2 gas for 150 min	[2]
Activated carbon + boric acid	Calcination at 500 °C in N_2 gas for 300 min	[3]
Activated carbon obtained from coal + borax decahydrate	Processed at 60 °C for 2 h and dry at 80 °C	[4]
Activated carbon obtained from coal + borax decahydrate	Processed at 40 °C for 2 h and dry at 80 °C	[5]
Activated carbon + water + sulfuric acid + boric acid	In vacuum at 80 °C	[6]
Activated carbon + helium + ammonia + borax decahydrate + water	Heat treatment in the furnace at 400 to 600 °C	[7]

2. Results and Discussion

According to the XRD analysis given in Figure 1, it can be seen that CAC material has an amorphous structure. In addition, two large broad peaks appearing near 2θ = 24° and 2θ = 42° can be noticed and they are attributed to reflections from (002) and (100) planes [8]. Many sharp diffraction peaks seen around 2θ = 30° to 40° are attributed to the presence of impurity elements and phases [9,10]. This may be due to the chemical activation materials used during the production of CAC material. The peaks between 2θ = 45° and 60° are the peaks of non-carbon materials originating from CAC production. The peaks around 65° are attributed to the formation of a graphitic C(002) structure, while the peaks at 2θ ≈ 62° are attributed to the graphitic structure. These peaks have been attributed to the amorphous structure in the literature [11,12].

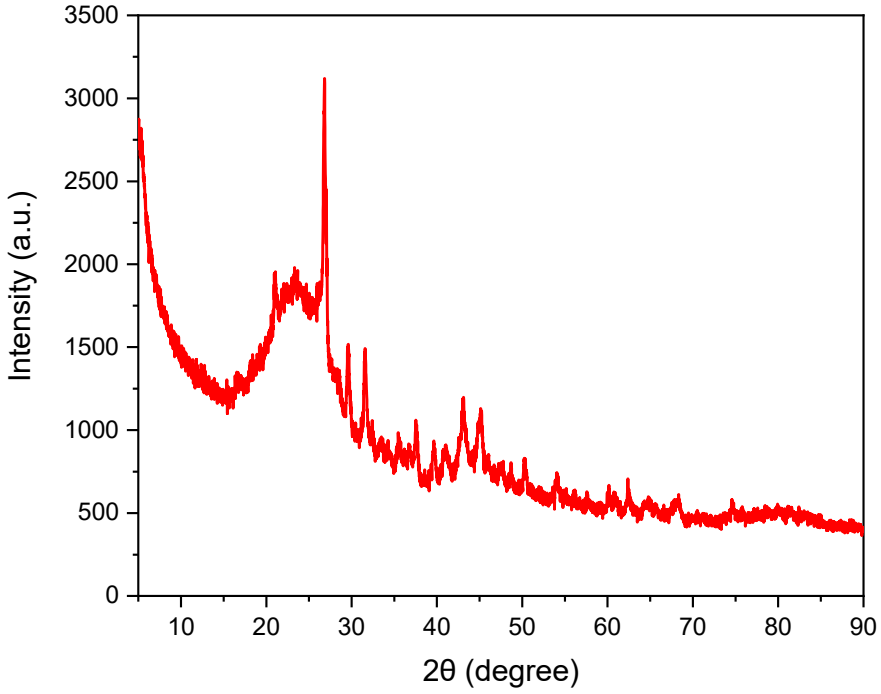


Figure 1. XRD patterns of commercial activated carbon.

The FTIR curves of CAC material are given in Figure 2. The peaks observed around 3600 are attributed to the O–H stretching mode, while the broad band between 1300 and 900 cm^{-1} with a maximum value at about 1100 cm^{-1} can be attributed to oxygenated functional groups. The absorption bands around 2850 and 2950 cm^{-1} represent the C–H and $–CH_2–$ stretching modes of aliphatic groups. The peaks observed around 1750 cm^{-1} are the absorption band for the carbonyl group and can be attributed to carboxylic acid groups [13]. In addition, the peaks observed between 1300 and 1456 cm^{-1} are identified as C–H bending vibrations, while the single points between about 1600 and 1500 cm^{-1} can be attributed to polar functional groups such as –OH [14]. It is thought that the peaks observed around 2345 cm^{-1} are due to the presence of C=C groups, and the peaks around 2085 cm^{-1} are related to C=N stretching vibrations. It has been stated that the band around 874 cm^{-1} is related to the stretching vibrations of the C–H out-of-plane band [15].

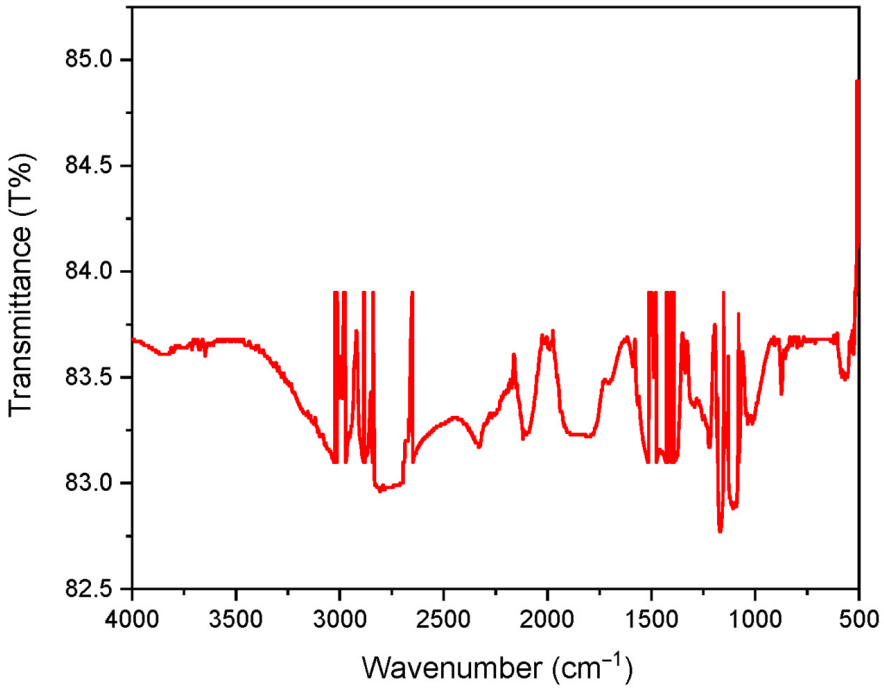


Figure 2. FTIR of commercial activated carbon.

The Raman curves of the CAC material are given in Figure 3. According to the Raman spectroscopy test, which is the most important technique in characterizing carbonaceous materials, the CAC material showed the D peak at approximately 1315 cm^{-1} and the G peak at 1588 cm^{-1}. These two peaks are the most intense peaks observed here. The D peak clearly revealed the presence of lattice defects, edge defects, disorganized alignment and a low-symmetry graphite structure in the CAC material. The G peak indicates the presence of C=C stretching vibrations. The degree of graphitization (R) was calculated using Equation (1) based on the intensities of the D and G peaks. Here, the intensity of the D peak is expressed as ID and the intensity of the G peak is expressed as IG [16].

$$\mathrm{R} = \frac{I_D}{I_G} \quad (1)$$

When the Raman data of the CAC material are applied to Equation (1), the RCAC is approximately 2.02 as calculated. This value is consistent with the material introduced as activated carbon obtained from the lignin of various biomasses (rice husk, flax, hemp and eucalyptus) in previous studies. However, this ratio shows that the CAC material does not have a regular lattice structure [17]. The broad peak peaking at approximately 2332 cm^{-1}

is due to the Raman mode of N_2 gas present in the air surrounding the sample [18]. The weak peaks observed between 2600 and 2700 cm^{-1} are referred to as 2D bands [19]. The 2D band indicates the presence of few-layer carbon material and a graphitic structure of the CAC material [16].

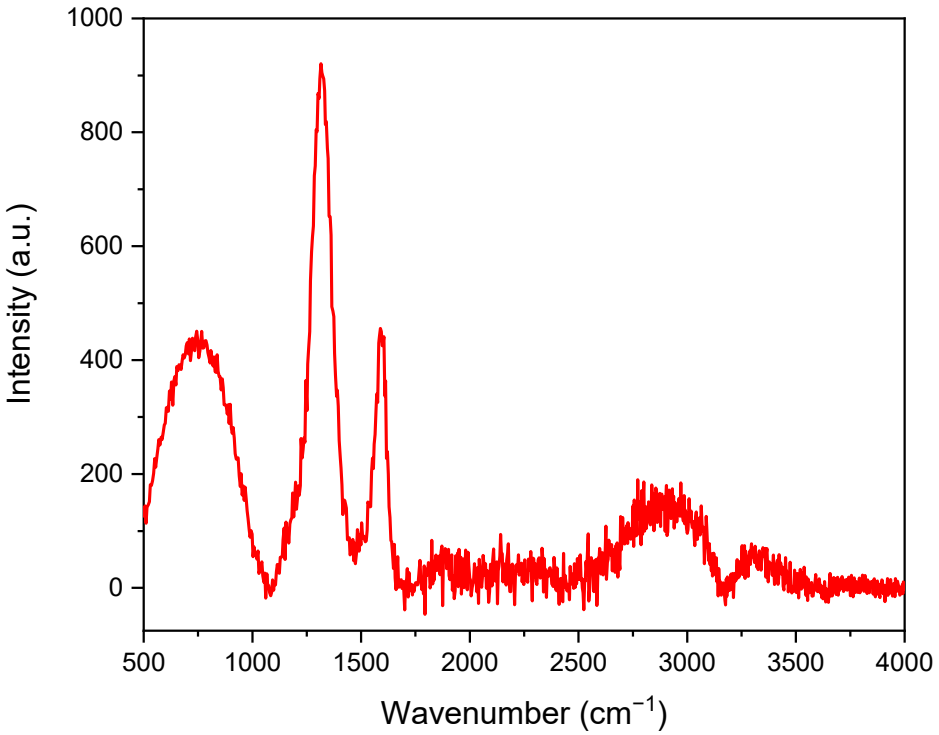


Figure 3. Raman plot of commercial activated carbon.

The FESEM images of CAC materials given in Figure 4 show that this material has a compact structure consisting of porous conglomerates and an irregular and rough profile with no standard size and shape. In addition, the rough structures and the presence of pores and indentations along the entire length of the material are quite evident [16,20]. EDS analyses show that the CAC material contains impurities consisting of elements such as Al, Si, S, K, Ca, Ti, and Fe. This information is particularly consistent with the XRD analyses. As can be understood from here, the impurity peaks seen in the XRD analysis can be attributed to these elements.

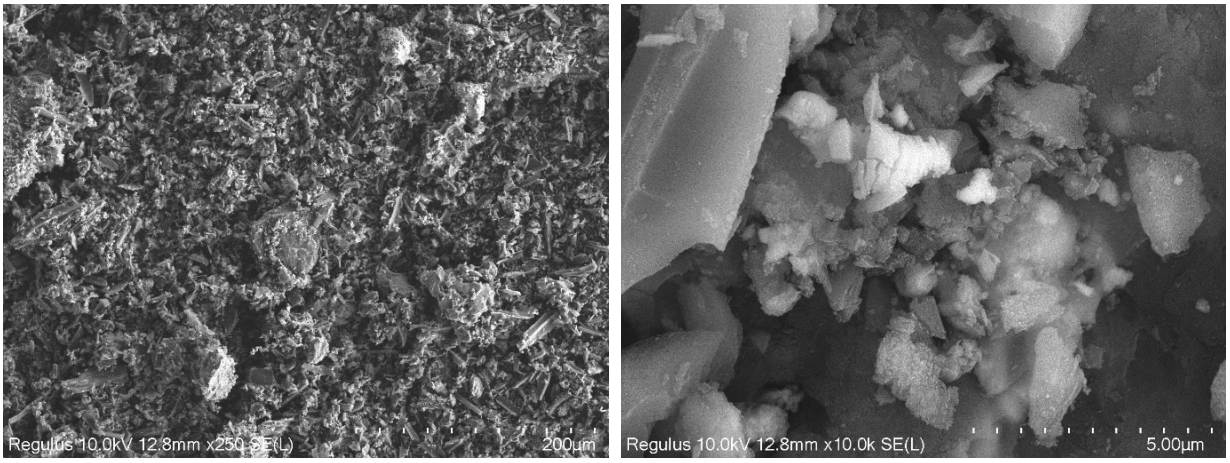
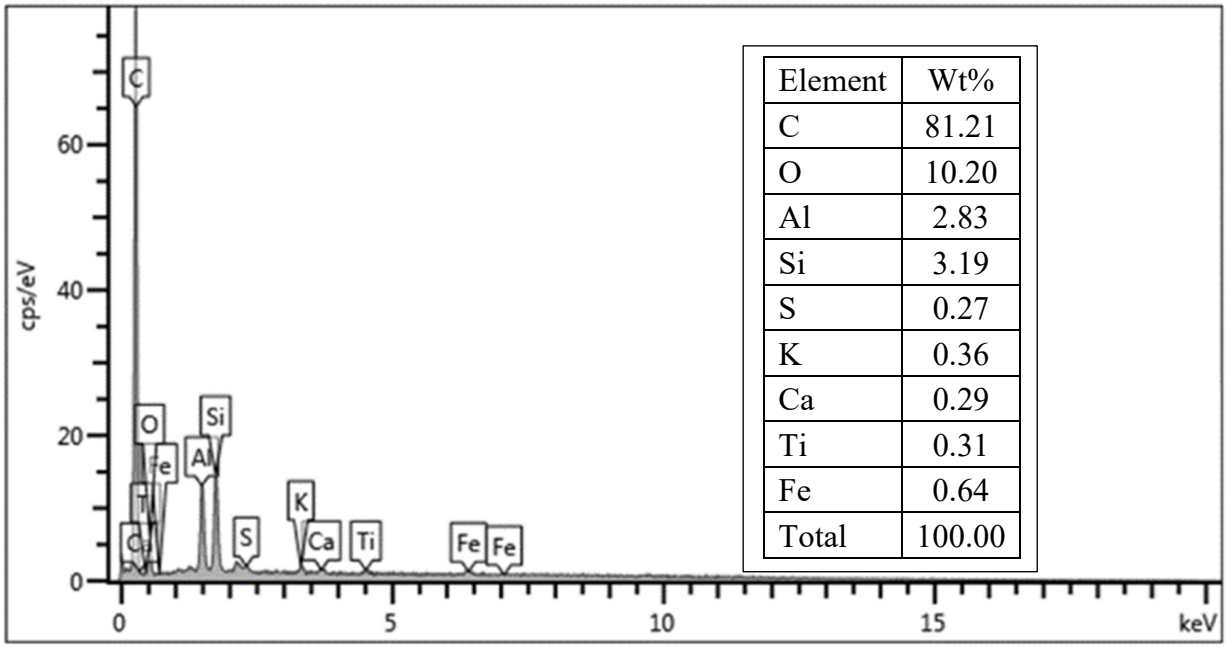


Figure 4. *Cont.*



Element	Wt%
C	81.21
O	10.20
Al	2.83
Si	3.19
S	0.27
K	0.36
Ca	0.29
Ti	0.31
Fe	0.64
Total	100.00

Figure 4. FESEM images and EDS results of commercial activated carbon.

Comparative XRD patterns of 0.25-BMCAC and 0.5-BMCAC materials are given in Figure 5. Consistent with previous studies [4], XRD analysis of boron-modified CAC samples showed broad and low diffraction peaks around 26° (002 plane) and 43° (100 plane), indicating the presence of an amorphous structure (43°) and disordered graphitic carbon (26°). In addition, sharp peaks seen at 2θ = 22° and 28°, broad peaks seen between 2θ = 22° and 28°, and broad peaks at 2θ = 42°~47° were identified as an amorphous carbon structure [21]. In addition, 0.25-BMCAC material exhibited generally more intense peaks at other carbon peaks, except the peak at 2θ = 28°, compared to 0.5-BMCAC material. The peaks observed at 2θ = 20.5°, 22.82°, 30.5°, 41.2°, 51° and 57.03° are attributed to borax material. This is in agreement with previous studies [22]. The presence of these peaks indicates further evidence of the presence of borax in boron-modified activated carbons.

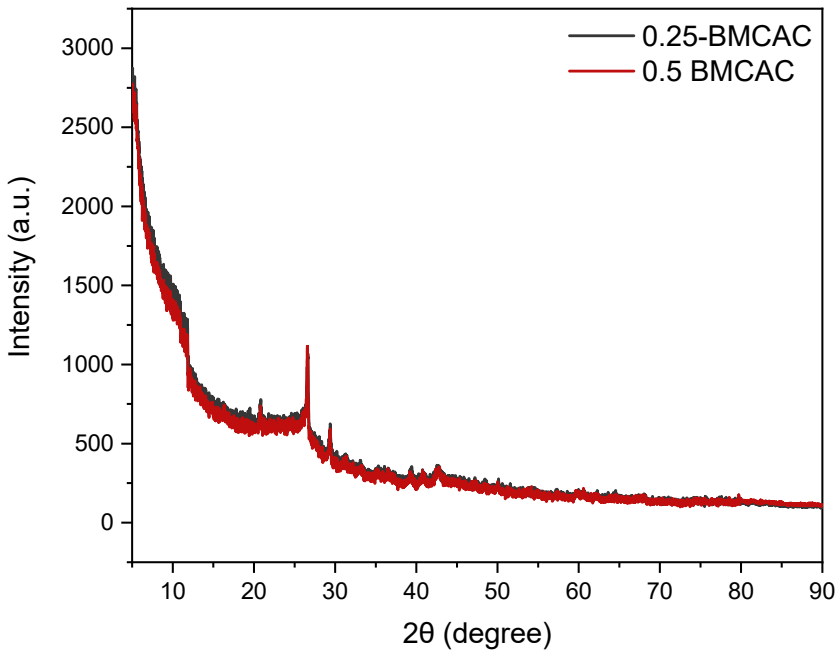


Figure 5. XRD patterns of boron-modified commercial activated carbons.

Comparative FTIR patterns of 0.25-BMCAC and 0.5-BMCAC materials are given in Figure 6, where 0.5-BMCAC exhibited a spectrum with sharper and more distinct peaks compared to 0.25-BMCAC material. The less intense peaks observed in 0.25-BMCAC were attributed to the formation of defects and the deterioration of the chemical structure. However, the band at about 925 cm^{-1} was attributed to B-H stretching, the 1025–1133 cm^{-1} mode to B-B stretching, and the 1362–1436 cm^{-1} mode to B-O stretching and oxy-functional groups. The band observed at about 1503 cm^{-1} shows the vibrations of the bending mode of BO_3, which may be due to the increased amount of oxygen groups. In addition, the moisture adsorbed due to the use of water while preparing the solutions of both materials showed itself around 1633 cm^{-1}. In addition, the peaks around 2332 and 2386 cm^{-1} represent B–H vibrations, the modes around 2850 and 2920 cm^{-1} show B–B (β12) characteristic bonding, and the broad peak around 3435 cm^{-1} indicates B–OH stretching [23]. The structures obtained in the FTIR analysis of the CAC material are also present here. Due to the presence of borax, the bands representing the structures of this material are more dominant. This confirmed that the CAC material induced phase composition and chemical bond modification as a result of modification with borax. In addition, the FTIR patterns in Figure 6 reveal that the induction of phase composition and chemical bond modification are more dominant depending on the increasing borax concentration.

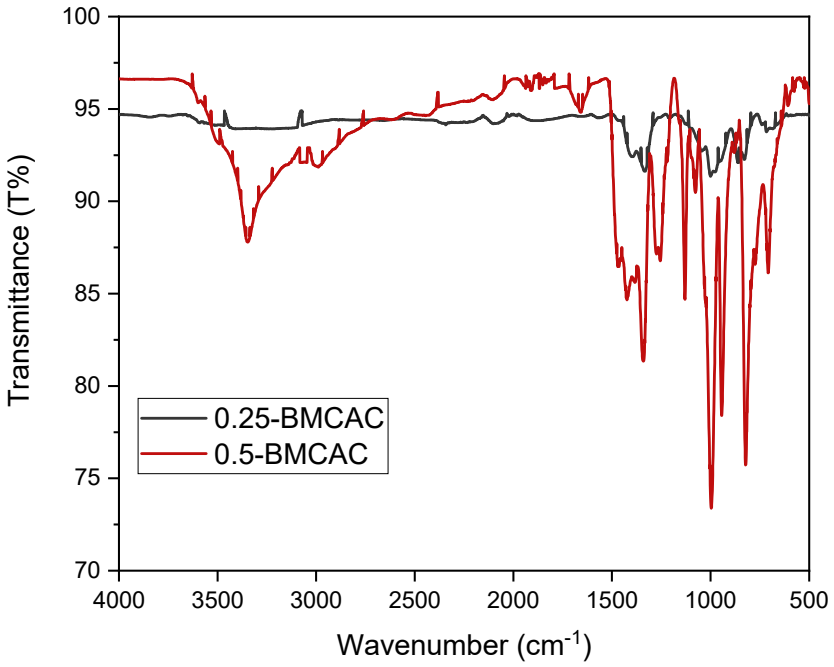


Figure 6. FTIR of boron-modified commercial activated carbons.

Figure 7 shows the Raman spectra of boron-modified activated carbon samples. On the other hand, 0.25-BMCAC material indicates D and G bands peaking at 1375 and 1593 cm^{-1}, respectively. It also shows a broad peak 2D band around it peaking at 2717 cm^{-1}, whereas 0.5-BMCAC material represents D and G bands at 1348 and 1606 cm^{-1}, respectively, and a broad peak 2D band peaking at 2735 cm^{-1}. All these are bands of the carbon material due to the presence of CAC material [16,24,25]. Furthermore, 0.25-BMCAC material showed a higher intensity of D and G bands and a lower intensity of 2D band compared to 0.5-BMCAC material. Due to increasing boron concentrations in 0.5-BMCAC, the intensity of D and G bands decreased and 2D bands increased. This may be an indicator of the phase composition and chemical bond modification of the borax material, which are consistent with the FTIR results. Using Equation (1), the R ratios of 0.25-BMCAC and 0.5-BMCAC

materials were calculated as ≈0.94 and ≈0.92, respectively. Considering the knowledge that there are fewer structural defects and other defects as the R ratio decreases in carbon-based materials [26], the order of the materials in this study are from the largest to the smallest in terms of structural defects and other defects as CAC > 0.25-BMCAC > 0.5-BMCAC. It is thought that the defects in the 0.25-BMCAC material, which has the most structural and other defects, may have been due to the insufficient bonding of the borax material with the carbon material or to the formation of weak bonds. It is thought that the material with higher borax content, 0.5-BMCAC, may have exhibited a less defective structure due to the stronger or more suitable ratio of bonds between boron and carbon atoms in it. This is another indication that the induction of phase composition and chemical bond modification has occurred, as consistent with FTIR tests. The broad bands seen in the range of approximately 500–750 cm^{-1} and 750–1000 cm^{-1} were attributed to the proven phases of boron compounds [27].

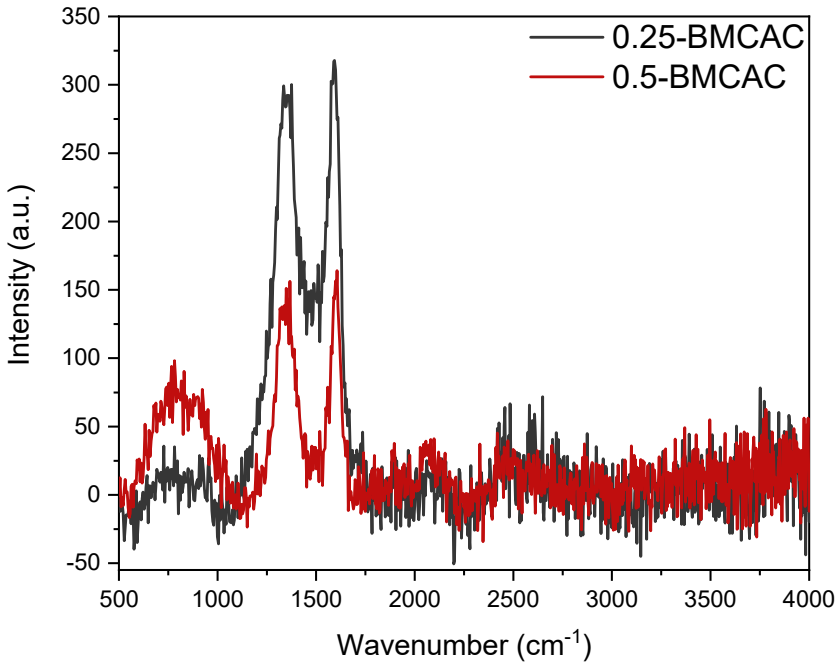
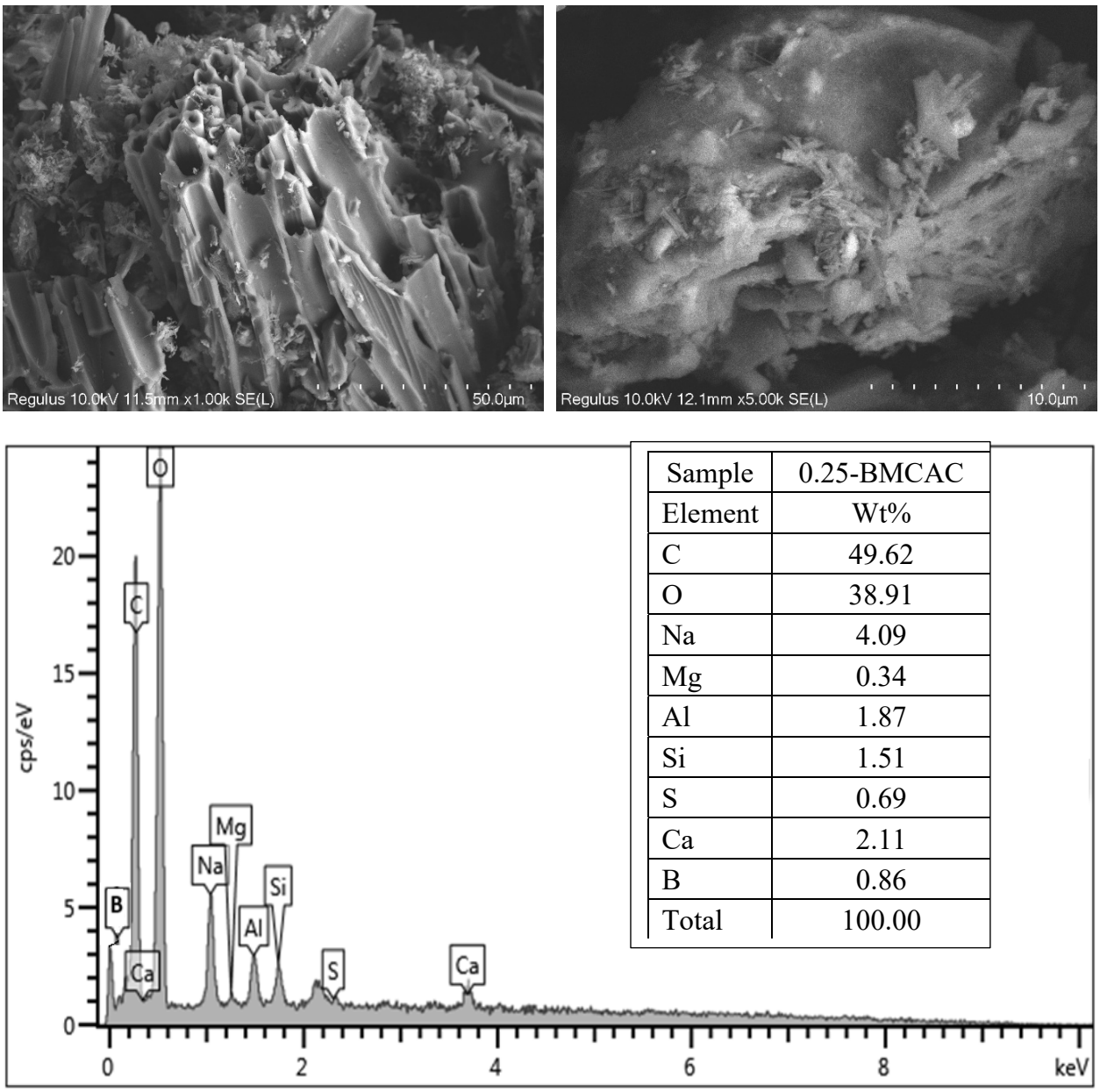


Figure 7. Raman plot of boron-modified commercial activated carbons.

The FESEM-EDS test findings of 0.25-BMCAC materials are presented in Figure 8. As can be seen, the porous tubular morphology and the porous tubular morphology are striking, which means that carbon retains distinct tunnel structures, as consistent with previous studies [25]. EDS analyses draw attention to the lower carbon content and much higher oxygen content compared to the CAC material. In addition, the presence of sodium element is normal in the structure of borax. These show that borax, a material with oxygen and sodium in its structure, is bound to the CAC surface as a result of the modification process [4,5]. This result is consistent with FTIR and Raman tests. The Mg, Al, Si, S, and Ca elements in EDS analyses are due to impurities found in the CAC material. Additionally, 0.25-BMCAC offers great potential for the development of new material technologies in the fields of environmental remediation, energy storage/conversion, lightweight compressible materials, and thermal insulation materials due to its porous tubular morphology structure [28]. Further studies are needed for the use of this material in the mentioned areas.



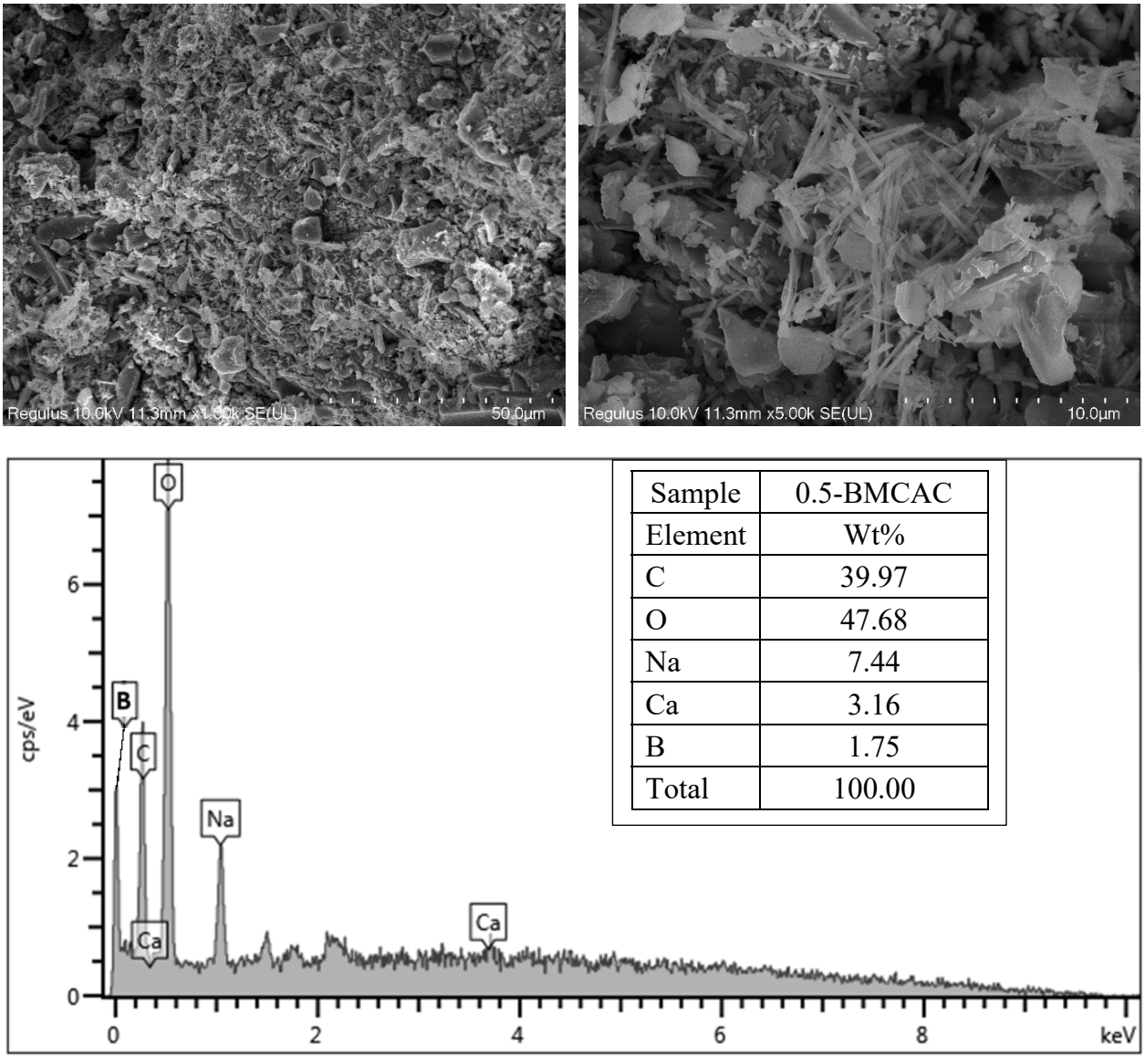
Sample	0.25-BMCAC
Element	Wt%
C	49.62
O	38.91
Na	4.09
Mg	0.34
Al	1.87
Si	1.51
S	0.69
Ca	2.11
B	0.86
Total	100.00

Figure 8. FESEM image and EDS result of 0.25 M boron-modified commercial activated carbon.

The FESEM-EDS test findings of 0.5-BMCAC materials are presented in Figure 9. Here, a compact, irregular and porous surface structure consisting of conglomerates is seen, lacking well-defined pores or surface features. However, in this example, the presence of wire-like structures of various micron lengths with increasing boron content is remarkable and indicates the formation of boron microwires [29,30]. The formation of these microwires can provide better strength (e.g., yield and tensile strength) for new composite materials to be made using this material. Therefore, it opens an important door for new and promising material research. In addition, it is thought that the absence of a tubular structure in 0.25-BMCAC is due to the closure of these structures due to increasing borax concentration. On the other hand, EDS results in both samples in the presence of impurities (elements such as Mg, Al, Si, S, Ca, etc.), confirming the XRD, FTIR, and Raman tests.

As a result, the characterization tests of CAC material consisting of XRD, FTIR, Raman, and FESEM-EDS gave consistent results, which revealed that CAC material contained non-carbon impurity elements and phases, and had a porous and disordered structure.

The characterization tests of 0.25-BMCAC and 0.5-BMCAC materials consisting of XRD, FTIR, Raman, and FESEM-EDS showed clearly that the amorphous structure of CAC material in these materials, as well as the induction of phase composition and chemical bond modification, was due to the borax modification process. It was also understood that the material with the most structural and other defects was the 0.25-BMCAC material and it was thought that these defects may be due to the insufficient bonding or weak bonding of borax material with carbon material. In addition, in the 0.25-BMCAC material, the porous tubular morphology means that the carbon has a distinct tunneled structures, while in the 0.5-BMCAC material, a compact, irregular, porous surface structure and the formation of boron microwires are remarkable.



Sample	0.5-BMCAC
Element	Wt%
C	39.97
O	47.68
Na	7.44
Ca	3.16
B	1.75
Total	100.00

Figure 9. FESEM image and EDS result of 0.5 M boron-modified commercial activated carbon.

3. Materials and Methods

3.1. Materials

Commercial activated carbon (CAC) produced from coconut shells with a particle size <200 mesh and originating from India was purchased from Beyanlab (İstanbul, Turkey). Borax decahydrate ($Na_2B_4O_7 \cdot 10H_2O$) material was purchased from Eti Mine Operations General Directorate (Ankara, Turkey). The distilled water used in the solution preparation

process was purchased from Onur Kimya Inc. (Ankara, Turkey). A magnetic stirrer (Weightlab WN-H320, İstanbul, Turkey) was used for solution mixing. Filter paper was used for filtration. The drying oven (Weightlab WF-HT125) was purchased from Lab Evreni Company (İstanbul, Turkey).

3.2. Preparation of Boron-Modified Activated Carbons

Inspired by previous studies [4], boron-modified activated carbon was prepared. For this purpose, two separate borax decahydrate solutions, 0.25 M and 0.5 M, were prepared in 100 mL of distilled water, which was used in all solution preparation processes. Each of these solutions was mixed with 2 g of CAC material at 60 °C for 2 h using a magnetic stirrer to obtain a homogeneous structure. The speed setting of the magnetic stirrer was found experimentally to ensure good and splash-free mixing, and since the maximum speed was determined as 500 rpm, all solutions were mixed at 500 rpm on the magnetic stirrer.

In the final stage, the samples were filtered using filter paper and the materials remaining on the filter paper were dried in the oven at 80 °C. After a 4 h drying process, two different boron-modified activated carbons were obtained. The sample prepared with 0.25 M borax solution was called 0.25-BMCAC, and the sample prepared with 0.5 M borax solution was called 0.5-BMCAC.

Two separate boron-modified activated carbon samples, the synthesis of which was completed, were subjected for characterization tests. The test results were analyzed and interpreted in light of the literature.

3.3. Characterization

In this study, material characterization tests consisting of XRD, FTIR, Raman spectroscopy (Raman test for short) and FESEM-EDS were performed to provide insight into the modification processes of commercial activated carbon material with borax. The XRD test was performed to provide an opportunity to understand the structural phases associated with the modification processes [1,7]. An FTIR test was performed to understand the surface modifications and functional groups [2]. Raman tests were performed due to their ability to show the degree of functionalization by comparing the intensities of D and G bands of carbon materials [4]. In addition, FESEM-EDS analyses were performed to understand the morphology and elemental structure of the samples [5].

XRD tests were performed by means of an APD 2000 PRO diffractometer instrument (Milan, Italy) using Cu Kα radiation (ß = 1.541840 Å) from a Cu X-ray tube operated at 30 kV and 10 mA [7]. FTIR tests were performed with diamond ATR spectrum analysis using an FTIR Spectrometer (PerkinElmer, Waltham, MA, USA, Spectrum Two). Raman tests were completed by obtaining spectra using the "Renishaw inVia Raman Microscope". FESEM-EDS analyses were performed using the Hitachi Regulus 8230 (Tokyo, Japan).

Structural characterization (XRD, FTIR, Raman, FESEM-EDS) tests were first applied to CAC then to 0.25-BMCAC and 0.5-BMCAC materials.

4. Conclusions

Boron-modified activated carbons were successfully prepared as a result of chemical modification processes using commercial activated carbon and borax solutions. It is confirmed in this study that commercial activated carbons have an amorphous structure and this material contains various impurity elements and phases. FTIR analysis of the CAC material showed various bonds and properties of carbon. According to the Raman analysis of the CAC material, lattice defects, edge defects, and C=C stretching vibrations are present in this material, and a several-layered structure and graphite structure are observed. The R ratio is about 2.02 and is consistent with the material introduced in the literature as

activated carbon obtained from lignin of various biomasses. Furthermore, FESEM images of CAC material indicate that it has an irregular and rough profile consisting of porous conglomerates because EDS analysis clearly reveals various impurities. This shows that XRD, FTIR, Raman, and FESEM-EDS analyses are consistent with each other. Comparative XRD patterns of 0.25-BMCAC and 0.5-BMCAC materials reveal carbon and borax peaks, providing evidence for the successful preparation of boron-modified activated carbons. On the other hand, 0.5-BMCAC material exhibits a peak at $2\theta = 28^{\circ}$, indicating the increase in the borax. FTIR analysis of boron-modified activated carbons shows that 0.5-BMCAC exhibits more pronounced boron bonds and bonding properties. It was also observed that the relationship between the increasing amount of oxygen groups and the amount of borax was reflected in the bond structures. The weak peaks in 0.25-BMCAC were associated with defect formation and the deterioration of the chemical structure. Raman analysis showed that the intensity of D and G bands decreased and the intensity of 2D bands increased with increasing boron concentration in 0.5-BMCAC. Additionally, 0.5-BMCAC has the lowest R ratio and it is the material with the fewest structural defects in this study. This indicates that the most suitable boron-modified activated carbon can be made using CAC and borax materials using 0.5 M borax solution. In this study, the structural characterization tests of boron-modified activated carbons are consistent with each other and clearly show the occurrence of the induction of phase composition and chemical bond modifications. The porous tubular morphology structure of 0.25-BMCAC holds great promise for the development of new material technologies in the fields of environmental remediation, energy storage/conversion, lightweight compressible materials, and thermal insulation materials. The morphology of 0.5-BMCAC, which shows the presence of microwires, offers significant potential to provide better strength (e.g., yield and tensile strength) for the construction of new composite materials.

Author Contributions: Conceptualization, I.D.; Methodology, I.D.; Formal analysis, N.Ç.; Investigation, N.Ç.; Resources, S.S.; Data curation, I.D.; Writing—original draft, N.Ç.; Writing—review & editing, A.O.; Visualization, S.S.; Supervision, A.O.; Funding acquisition, S.S. All authors have read and agreed to the published version of the manuscript.

Funding: This research received no external funding.

Data Availability Statement: The original contributions presented in this study are included in the article. Further inquiries can be directed to the corresponding author.

Acknowledgments: We would like to thank the Gazi University Photonics Research and Application Center for their support in performing XRD tests. We would like to thank the Eskişehir Osmangazi University Center Research Laboratory Application and Research Center for supporting us in performing FTIR, Raman and FESEM-EDS tests. The authors would like to thank the KARDEMİR Advanced Technologies Research and Engineering Center for their assistance in the use of laboratory equipment.

Conflicts of Interest: Author Ismail Demir was employed by the company Karabuk Iron and Steel Factories (KARDEMİR) Inc. The remaining authors declare that the research was conducted in the absence of any commercial or financial relationships that could be construed as a potential conflict of interest.

References

1. Romanos, J.; Beckner, M.; Stalla, D.; Tekeei, A.; Suppes, G.; Jalisatgi, S.; Lee, M.; Hawthorne, F.; Robertson, J.D.; Firlej, L.; et al. Infrared study of boron–carbon chemical bonds in boron-doped activated carbon. *Carbon* **2013**, *54*, 208–214. [CrossRef]
2. Ganiyu, S.A.; Ajumobi, O.O.; Lateef, S.A.; Sulaiman, K.O.; Bakare, I.A.; Qamaruddin, M.; Alhooshani, K. Boron-doped activated carbon as efficient and selective adsorbent for ultra-deep desulfurization of 4,6-dimethyldibenzothiophene. *Chem. Eng. J.* **2017**, *321*, 651–661. [CrossRef]

3. Jia, Y.; Hu, R.; Zhou, Q.; Wang, H.; Gao, X.; Zhang, J. Boron-modified activated carbon supporting low-content Au-based catalysts for acetylene hydrochlorination. *J. Catal.* **2017**, *348*, 223–232. [CrossRef]
4. Kopac, T.; Kırca, Y.; Toprak, A. Synthesis and characterization of KOH/boron modified activated carbons from coal and their hydrogen sorption characteristics. *Int. J. Hydrogen Energy* **2017**, *42*, 23606–23616. [CrossRef]
5. Kopac, T.; Kırca, Y. Effect of ammonia and boron modifications on the surface and hydrogen sorption characteristics of activated carbons from coal. *Int. J. Hydrogen Energy* **2020**, *45*, 10494–10506. [CrossRef]
6. Chen, X.; Wang, L.; Sun, W.; Yang, Z.; Jin, J.; You, D.; Liu, G. Enhanced electrochemical advanced oxidation on boride activated carbon: The influences of boron groups. *Electrochim. Acta* **2021**, *400*, 139462. [CrossRef]
7. Morandé, A.; Lillo, P.; Blanco, E.; Pazo, C.; Dongil, A.B.; Zarate, X.; Saavedra-Torres, M.; Schott, E.; Canales, R.; Videla, A.; et al. Modification of a commercial activated carbon with nitrogen and boron: Hydrogen storage application. *J. Energy Storage* **2023**, *64*, 107193. [CrossRef]
8. Wang, S.; Nam, H.; Gebreegziabher, T.B.; Nam, H. Adsorption of acetic acid and hydrogen sulfide using NaOH impregnated activated carbon for indoor air purification. *Eng. Rep.* **2020**, *2*, e12083. [CrossRef]
9. Zhang, L.; Yuan, J.; Su, S.; Cui, Y.; Shi, W.; Zhu, X. Porous active carbon derived from lotus stalk as electrode materialfor high-performance supercapacitors. *J. Wood Chem. Technol.* **2021**, *41*, 46–57. [CrossRef]
10. Wu, Z.; Liu, Y.; Xu, Y.; Zhan, W.; Liu, Y.; Zhang, D.; Xu, Y. Preparation of activated carbon through the pyrolysis of waste bamboo chips and evaluation of its CO_2 adsorption efficacy. *Biomass Convers. Biorefinery* **2024**, *ahead of print*. [CrossRef]
11. Kristianto, H.; Arie, A.A.; Susanti, R.F.; Halim, M.; Lee, J.K. The effect of activated carbon support surface modification on characteristics of carbon nanospheres prepared by deposition precipitation of Fe-catalyst. *IOP Conf. Ser. Mater. Sci. Eng.* **2016**, *162*, 012034. [CrossRef]
12. Van, H.T.; Nguyen, T.M.P.; Thao, V.T.; Vu, X.H.; Nguyen, T.V.; Nguyen, L.H. Applying Activated Carbon Derived from Coconut Shell Loaded by Silver Nanoparticles to Remove Methylene Blue in Aqueous Solution. *Water Air Soil Pollut.* **2018**, *229*, 393. [CrossRef]
13. Nieto-Delgado, C.; Rangel-Mendez, J.R. Production of activated carbon from organic by-products from the alcoholic beverage industry: Surface area and hardness optimization by using the response surface methodology. *Ind. Crops Prod.* **2011**, *34*, 1528–1537. [CrossRef]
14. Yang, Z.; Gleisner, R.; Mann, D.; Xu, J.; Jiang, J.; Zhu, J.Y. Lignin Based Activated Carbon Using H3PO4 Activation. *Polymers* **2020**, *12*, 2829. [CrossRef]
15. Mojoudi, N.; Mirghaffari, N.; Soleimani, M.; Shariatmadari, H.; Belver, C.; Bedia, J. Phenol adsorption on high microporous activated carbons prepared from oily sludge: Equilibrium, kinetic and thermodynamic studies. *Sci. Rep.* **2019**, *9*, 19352. [CrossRef]
16. Gupta, G.K.; Sagar, P.; Pandey, S.K.; Srivastava, M.; Singh, A.K.; Singh, J.; Srivastava, A.; Srivastava, S.K.; Srivastava, A. In Situ Fabrication of Activated Carbon from a Bio-Waste Desmostachya bipinnata for the Improved Supercapacitor Performance. *Nanoscale Res. Lett.* **2021**, *16*, 85. [CrossRef]
17. Rowlandson, J.L.; Edler, K.J.; Valeska, M.T.; Ting, P. Toward Process-Resilient Lignin-Derived Activated Carbons for Hydrogen Storage Applications. *ACS Sustain. Chem. Eng.* **2020**, *8*, 2186–2195. [CrossRef]
18. Zappielo, C.D.; Nanicuacua, D.M.; Santos, W.N.L.D.; da Silva, D.L.F.; Dall'Antônia, L.H.; de Oliveira, F.M.; Clausena, D.N.; Tarley, C.R.T. Solid Phase Extraction to On-Line Preconcentrate Trace Cadmium Using Chemically Modified Nano-Carbon Black with 3-Mercaptopropyltrimethoxysilane. *J. Braz. Chem. Soc.* **2016**, *27*, 1715–1726. [CrossRef]
19. Li, Z.; Deng, L.; Kinloch, I.A.; Young, R.J. Raman spectroscopy of carbon materials and their composites: Graphene, nanotubes and fibres. *Prog. Mater. Sci.* **2023**, *135*, 101089. [CrossRef]
20. Li, P.-H.; Wu, W.-J. Co-doping mechanism of biomass-derived nitrogen-boron porous carbon and its applications in energy storage and environmental purification. *J. Alloys Compd.* **2024**, *1002*, 175098. [CrossRef]
21. Wang, H.; Li, Z.; Yahyaoui, S.; Hanafy, H.; Seliem, M.K.; Bonilla-Petriciolet, A.; Dotto, G.L.; Sellaoui, L.; Li, Q. Effective adsorption of dyes on an activated carbon prepared from carboxymethyl cellulose: Experiments, characterization and advanced modelling. *Chem. Eng. J.* **2021**, *417*, 128116. [CrossRef]
22. Gumus, O.Y.; Unal, H.I.; Erol, O.; Sari, B. Synthesis, characterization, and colloidal properties of polythiophene/borax conducting composite. *Polym. Compos.* **2011**, *32*, 418–426. [CrossRef]
23. Zielinkiewicz, K.; Baranowska, D.; Mijowska, E. Ball milling induced borophene flakes fabrication. *RSC Adv.* **2023**, *13*, 16907–16914. [CrossRef] [PubMed]
24. Devarajan, J.; Arumugam, P. Boron-doped activated carbon from the stems of Prosopis juliflora as an effective electrode material in symmetric supercapacitors. *J. Mater. Sci. Mater. Electron.* **2022**, *33*, 17469–17482. [CrossRef]
25. Pardanaud, C.; Aréou, E.; Martin, C.; Ruffe, R.; Angot, T.; Roubin, P.; Hopf, C.; Schwarz-Selinger, T.; Jacob, W. Raman micro-spectroscopy as a tool to measure the absorption coefficient and the erosion rate of hydrogenated amorphous carbon films heat-treated under hydrogen bombardment. *Diam. Relat. Mater.* **2012**, *22*, 92–95. [CrossRef]

26. Qian, X.; Wang, X.; Zhong, J.; Zhi, J.; Heng, F.; Zhang, Y.; Song, S. Effect of fiber microstructure studied by Raman spectroscopy upon the mechanical properties of carbon fibers. *J. Raman Spectrosc.* **2019**, *50*, 665–673. [CrossRef]
27. Sasidharanpillai, S.; Arcis, H.; Trevani, L.; Tremaine, P.R. Triborate Formation Constants and Polyborate Speciation under Hydrothermal Conditions by Raman Spectroscopy using a Titanium/Sapphire Flow Cell. *J. Phys. Chem. B* **2019**, *123*, 5147–5159. [CrossRef]
28. Sun, J.; Wu, Z.; Ma, C.; Xu, M.; Luo, S.; Li, W.; Liu, S. Biomass-derived tubular carbon materials: Progress in synthesis and applications. *J. Mater. Chem. A* **2021**, *9*, 13822–13850. [CrossRef]
29. Wu, Y.; Liu, Y.; Kuang, Z.; Hussain, M.; Yang, W.; Zhou, C.; Wu, G. High-quality boron carbide nanowires prepared by catalyst-free template growth method. *Ceram. Int.* **2022**, *48*, 21846–21855. [CrossRef]
30. Avcıoğlu, S.; Kaya, F.; Kaya, C. Morphological evolution of boron carbide particles: Sol-gel synthesis of nano/micro B_4C fibers. *Ceram. Int.* **2021**, *47*, 26651–26667. [CrossRef]

Disclaimer/Publisher's Note: The statements, opinions and data contained in all publications are solely those of the individual author(s) and contributor(s) and not of MDPI and/or the editor(s). MDPI and/or the editor(s) disclaim responsibility for any injury to people or property resulting from any ideas, methods, instructions or products referred to in the content.